

## Adsorption of vancomycin antibiotic from aqueous solution using an activated carbon impregnated magnetite composite

Forough Gashtasbi<sup>a,b</sup>, Reza Jalilzadeh Yengejeh<sup>b,\*</sup>, Ali Akbar Babaei<sup>c,d</sup>

<sup>a</sup>Department of Environmental Engineering, Khuzestan Science and Research Branch, Islamic Azad University, Ahvaz, Iran, email: foroughgashtasbi@yahoo.com

<sup>b</sup>Department of Environmental Engineering, Ahvaz Branch, Islamic Azad University, Ahvaz, Iran, Tel. +00-989-124794322, email: r.jalilzadeh@iauahvaz.ac.ir

<sup>c</sup>Environmental Technologies Research Center, Ahvaz Jundishapur University of Medical Sciences, Ahvaz, Iran, email: babaei-a@ajums.ac.ir

<sup>d</sup>Department of Environmental Health Engineering, School of Public Health, Ahvaz Jundishapur University of Medical Sciences, Ahvaz, Iran

Received 25 February 2017; Accepted 9 September 2017

### ABSTRACT

Vancomycin antibiotic is one of the most common antibiotics in hospitals in different parts of the world. The aim of this research was to synthesize a powder activated carbon impregnated magnetite composite (PAC/Fe<sub>3</sub>O<sub>4</sub>) for vancomycin removal from aqueous solution. The physical, chemical and surfaces characteristics of the synthesized composite were determined using XRD, SEM, VSM and BET techniques. Furthermore, several batch experiments were carried out to find vancomycin adsorption onto the PAC/Fe<sub>3</sub>O<sub>4</sub> under various input variables namely, pH of aqueous media, reaction time, adsorbent dosages and initial antibiotic concentrations. In addition, isotherm and kinetic studies of antibiotic adsorptive removal were carried out using various models. Results showed that the maximum amount of vancomycin adsorption (97.83%) was obtained at pH of 5 during 60 min. Moreover, the direct and indirect relationships were observed between antibiotic removal and adsorbent dosage and initial antibiotic concentration, respectively. Furthermore, the obtained results of isotherm and kinetic studied revealed that Freundlich isotherm model and pseudo second-order kinetic model had the highest correlation with the experimental data of antibiotic adsorption. Finally, the reusability experiments showed that PAC/Fe<sub>3</sub>O<sub>4</sub> cannot only has high ability of antibiotic adsorption, but also has high stability after five cycles of application.

*Keywords:* Adsorption; Isotherm; Kinetic; Magnetite composite; Vancomycin

### 1. Introduction

The presence of antibiotics in aqueous solution as new pollutants has extensively drawn the attention of lots of environmentalists [1,2]. Antibiotics were produced for treatment of infectious diseases in veterinary science and also prescribed for human diseases. Antibiotics with complicated structures, low degradability, high toxicity and mutagenic features have been recognized as one of

the most serious challenges in environmental remediation perspectives [3,4]. In Germany, around 20-40% of all antibiotics are discharged directly [5]. Research showed that most of wastewater treatment techniques are capable of removing 60-90% of antibiotics, while the residuals depleted into the environmental resources such as surface and ground waters, sludge and soils [6–8]. Up to now, lots of antibiotics like tetracycline, amoxicillin, penicillin, vancomycin and ciprofloxacin have been recognized in wastewaters [9]. Vancomycin is an antibiotic which is categorized in Beta-Lactam and Glycopeptide antibiotic group which is derived

\*Corresponding author.

from amycolatopsis orientalis bacteria. The chemical structure of vancomycin is demonstrated in Fig. 1.

Until now, several remediation approaches such as advanced oxidation process (e.g., ozonation [10,11], application of UV and chemical oxidants like potassium ferrate, permanganate which can generate hydroxyl (OH) ions [12–14], membrane processes [15], adsorption [16] and biodegradation [17] have been applied to remove antibiotics from aqueous solution. The aforementioned methods are not potentially cost-effective, efficient and environmental friendly, due to the toxicity to the microorganisms and production of toxic substances such as ozone, trihalomethanes and halogens [18,19]. Therefore, finding an effective and economic method for treatment of wastewater containing antibiotic is quite necessary.

Over the past few decades, the adsorption has widely been applied, due to the cost-effectiveness, ease of adsorbent preparation and high efficiency. Recently, environmentalists have focused on the preparation and application of raw and cheap adsorbents which obtained from cheap and highly available raw materials and do not produce secondary pollution [20,21]. Activated carbon (AC) with specific structure, high adsorption capacity, bioavailability and lack of production of toxic secondary substances (e.g. ozone and radicals) has extensively been used as an efficient and promising adsorbent for removal of non-biodegradable pollutants in aqueous solution [22,23]. Previous research has shown that cheap adsorbents had high ability to remove antibiotics from solution. For example, Legnoverde et al. [24] reported that SBA-15 mesoporous silica could efficiently increase cephalixin removal from aqueous solution. Furthermore, results of Pouretedal and Sadegh [22] revealed that the activated carbon obtained from vine wood had high capability of adsorbing antibiotics in solution. However, one of the most common operational problems in the application of AC is its separation from aqueous solution, after reaction with contaminants, due to their small size and high dispersivity [21]. Therefore, magnetization has been suggested as an

effective approach to separate AC from aqueous solution that not only leads to their separation via an external magnet, but also decrease the cost of filtration process [25]. In addition, the impregnation of surfactants, polymers and porous materials with magnetite nanoparticles has led to increasing the dispersivity of nanoparticles in aqueous solution and enhancing their removal efficiency [26]. Esfahani and Firouzi [27] reported that the application of sepiolite for modification of zero-valent iron nanoparticles (ZVIN) caused a significant increase in their ability to remove hexavalent chromium (Cr(VI)) from aqueous solution. In another study, Do et al. [28] reported that activated carbon had high capability of increasing the performance of magnetite nanoparticles to remove methyl orange from aqueous solution.

Although antibiotic removal using cheap adsorbents have widely been studied, the adsorption of vancomycin onto the PAC/Fe<sub>3</sub>O<sub>4</sub> has not been studied well. Hence, the main objectives of this paper were synthesis of an activated carbon impregnated magnetite nanocomposite and its application for vancomycin adsorptive removal from aqueous solution at different experimental variables. Moreover, some selected isotherm and kinetic studies were applied to fit the experimental data of vancomycin adsorptive removal in order to find the most suitable models. Finally, the reusability experiments were carried out to evaluate the efficiency of PAC/Fe<sub>3</sub>O<sub>4</sub> after some cycles of use.

## 2. Materials and methods

### 2.1. Chemicals

Raw antibiotic powder was purchased from Jaber Ebne Hayyan Pharmaceutical Company. While, concentrated hydrochloric acid (12 N HCl) and sodium hydroxide (NaOH) were prepared from Merck Co, Germany. Antibiotic stock solution (1000 mg/L) was prepared by addition of 0.1 g

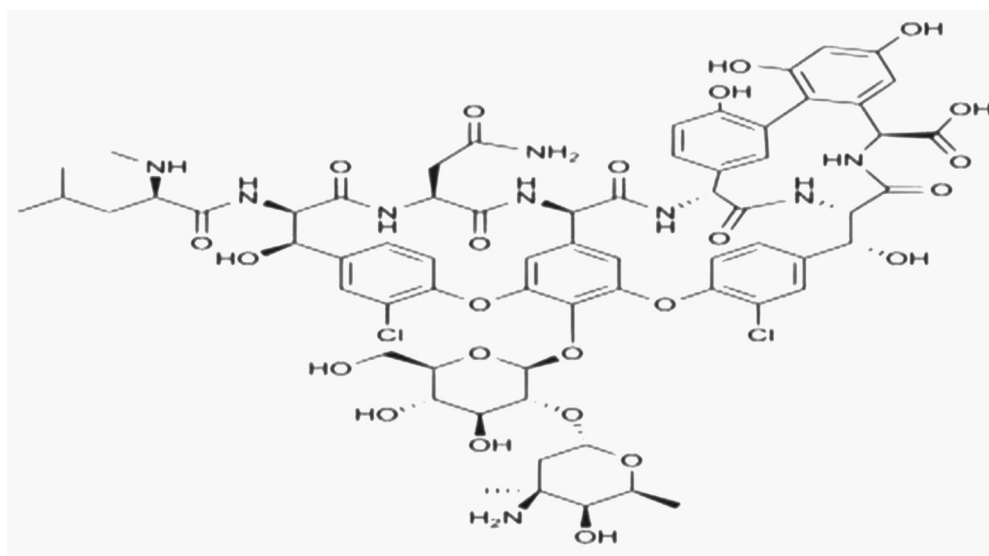


Fig. 1. Chemical structure of vancomycin.

antibiotic powder to 100 mL of Deionized (DI) water. Then, the required concentrations were obtained by dilution. All solutions were kept at 4°C, prior to the experiments.

## 2.2. Synthesis of composite

In this research, PAC/Fe<sub>3</sub>O<sub>4</sub> composite was synthesized using co-precipitation method proposed by Kakavandi et al. [25]. In brief, 0.5 activated carbon powder was added to 20 mL 65% nitric acid and kept in an ultrasonic bath at 80°C for 3 h to create a homogenized suspension. Then, the filtered carbon was added into the ferric iron solution and kept in an ultrasonic bath for 1 h. Afterwards, 28% ammonium solution was added dropwisely into the solution until dissolved iron was deposited as a magnetite. After filtration, the obtained powder was kept in an electrical furnace for 3 h at 750°C. The synthesized composite was separated using an external magnet, washed sequentially with DI water, dried in an oven at 105°C overnight and kept in a desiccator.

Size, morphology and surface characteristics of the synthesized composite were determined using a scanning electron microscope (SEM, Philips, XL30). The crystalline features of PAC/Fe<sub>3</sub>O<sub>4</sub> were found using X-ray diffraction technique (XRD, Quantachrome, 2000, NOVA). Furthermore, electron dispersive X-ray (EDX) technique was applied to characterize the elemental analysis of the synthesized composite. The specific surface area of composite was determined using BET method (Quantachrome, 2000, NOVA). Finally, the magnetic features of PAC/Fe<sub>3</sub>O<sub>4</sub> were characterized using a vibrating sample magnetometer (VSM) (7400, Lakeshore, USA) at room temperature (25 ± 2°C).

## 2.3. Batch experiments

The adsorption study of vancomycin onto the surfaces of PAC/Fe<sub>3</sub>O<sub>4</sub> was performed in a series of batch experiments under different input variables such as pH of solution (3–11), contact time (2–120 min), adsorbent dosages (0.1–2 g/L) and initial antibiotic concentrations (10–100 mg/L). Therefore, various dosages of adsorbent were added into the 250 mL experimental tubes containing 100 mL of antibiotic solution. Then, the bottles were shaken on a rotary shaker at different time intervals at room temperature (25 ± 2°C). After completion the reaction, the solution was passed through a filter paper (watman 42. no) and the adsorbent particles were separated from the solution using a strong magnet. Finally, the residual antibiotic concentrations in the solution were determined using a UV-visible spectrophotometer at the wavelength of 240 nm. The antibiotic removal efficiency (R%) and adsorption capacity (q<sub>i</sub>) were calculated via the equations below:

$$R = \frac{C_0 - C}{C_0} \times 100 \quad (1)$$

$$q_i = \frac{(C_0 - C)V}{W} \quad (2)$$

where C<sub>0</sub> and C are the initial and residual antibiotic concentrations (mg/L), respectively. V is the volume of solution (L) and W is the mass of adsorbent (g).

## 2.4. Isotherm and kinetic studies

### 2.4.1. Adsorption isotherm

For finding the adsorption parameters, the analysis of isotherm data is of great importance. Therefore, the experimental data of antibiotic adsorption were fitted on four commonly used isotherm model namely, Langmuir, Freundlich, Temkin and Dubinin-Radushkevich (D-R) to evaluate the adsorption parameters.

Langmuir isotherm model assumes that the process of adsorption of adsorbate molecules onto the reactive surface of the homogeneous adsorbent surface is monolayer and the adsorption process has the similar adsorption activation energy [29]. Equation below shows the linear form of Langmuir isotherm model as follows:

$$\frac{C_e}{q} = \frac{1}{K_L q_e} + \frac{C_e}{q_e} \quad (3)$$

where C<sub>e</sub> (mg/L) and q (mg/g) are the equilibrium antibiotic concentration and equilibrium amounts of adsorption, respectively. q<sub>e</sub> (mg/g) is the maximum adsorption capacity of antibiotic and K<sub>L</sub> is also the Langmuir equilibrium constant.

Freundlich is a useful isotherm model for both monolayer and multilayer adsorption and assumes that the adsorption is occurred onto the heterogeneous surface of the adsorbent [30]. The linear form of Freundlich model is given in the equation below:

$$\log q_e = \log K_F + \frac{1}{n} \log C_e \quad (4)$$

where K<sub>F</sub> and n are Freundlich equilibrium constant.

Temkin isotherm is defined based on a linear decline in adsorption energy because of the interaction between adsorbent and adsorbate [31]. The equation below demonstrates the linear form of Temkin model:

$$q_e = \frac{RT}{b} \ln K_T + \frac{RT}{b} \ln C_e \quad (5)$$

where R is the universal gas constant (8.314 J/mol·k), K<sub>T</sub> is Temkin equilibrium constant (L/g) and b is model constant related to the heat of sorption (J/mol). The linear form of Dubinin-Radushkevich (D-R) isotherm model is expressed as follows [32]:

$$\ln q_e = \ln q_d - \beta \varepsilon^2 \quad (6)$$

where q<sub>d</sub> is D-R model constant (mg/g), β is the model constant attributed to the free energy and ε is the Polanyi potential that is defined as below:

$$\varepsilon = RT \ln \left[ 1 + \frac{1}{C_e} \right] \quad (7)$$

#### 2.4.2. Adsorption kinetic

Kinetic study is an important tool for gaining some information on the physical chemistry of removal process and choosing the optimum experimental conditions in order to design a typical adsorption system. Hence, in this study, we fitted the adsorption data of antibiotic onto the surfaces of PAC/Fe<sub>3</sub>O<sub>4</sub> on four kinetic models.

The linear form of pseudo first-order kinetic model is expressed below [33]:

$$\log(q_e - q_t) = \log q_e - \frac{k_1}{2.303} t \quad (8)$$

The equation below gives the linear form of pseudo second-order kinetic model [34]:

$$\frac{t}{q_t} = \frac{1}{k_2 q_e^2} + \frac{t}{q_e} \quad (9)$$

The linear form of Elovich model is also given in the equation below [35]:

$$q_t = \frac{1}{\beta} \ln(\alpha\beta) + \frac{1}{\beta} \ln(t) \quad (10)$$

Finally, the linear form of intraparticle diffusion kinetic model can be expressed as follows:

$$q_t = k_{id} t^{0.5} + I \quad (11)$$

### 3. Results and discussion

#### 3.1. Characterization of composite

Fig. 2a and 2b show SEM image of PAC and PAC/Fe<sub>3</sub>O<sub>4</sub> indicating its porous structure with uniform pores and irregularities on the surfaces of the synthesized composite. Furthermore, the size of PAC/Fe<sub>3</sub>O<sub>4</sub> is in the range of 30–80 nm with cubic structure. Apparently, the lower particle size, the higher ability of adsorbent to remove contaminants. Furthermore, XRD diagrams of PAC, Fe<sub>3</sub>O<sub>4</sub> and PAC/Fe<sub>3</sub>O<sub>4</sub> which was performed at 2θ range of 10 and 70° are illustrated in Fig. 2c. Accordingly, a narrow and broad peak at 2θ of 25°C of XRD diagram of PAC was illustrated than shows the its amorphous nature. In addition, the XRD patterns of Fe<sub>3</sub>O<sub>4</sub> and PAC/Fe<sub>3</sub>O<sub>4</sub> were quite similar to each other the confirms the impregnation of PAC with nanoparticles. In fact, in the XRD pattern on of nanoparticles six peaks were seen at 2θ of 30.07°, 35.44°, 43.15°, 54.6°, 56.99°, and 62.6° corresponding to cubic phase Fe<sub>3</sub>O<sub>4</sub>. Similar peaks were also observed at XRD pattern of PAC/Fe<sub>3</sub>O<sub>4</sub> without significant changes that shows the successful synthesis of composite. Similar results are reported in previous studies [36,37]. The EDX spectrum of PAC/Fe<sub>3</sub>O<sub>4</sub> is also depicted in Fig. 2d. Based on the figure, the major elements in the body of composite are C (77.8%), O (4.9%) and Fe (16.3%) that confirms the bonding between magnetite and activated carbon. Fig. 2e represents the VSM magnetization curve of

PAC/Fe<sub>3</sub>O<sub>4</sub> at 25°C in the cycling magnetic field of –10 kOe to +10 kOe. The magnetization value of PAC/Fe<sub>3</sub>O<sub>4</sub> is 6.94 emu/g demonstrating an extraordinary magnetic response to a magnetic field. In addition, findings of BET analysis revealed that the average pore size of composite is 3.5 nm. According to the IUPAC classification, (micropores (*d* < 2 nm), mesopores (2 < *d* < 50 nm) and macropores (*d* > 50 nm)), so this composite can be categorized as mesoporous (Fig. 2f). The specific surface area of the composite is 857 m<sup>2</sup>/g which is higher than raw activated carbon powder (671.2 m<sup>2</sup>/g), indicating the role of existence of metal oxide onto the structure of AC.

#### 3.2. A comparative study

The adsorptive removal of vancomycin was performed using PAC, Fe<sub>3</sub>O<sub>4</sub> and PAC/Fe<sub>3</sub>O<sub>4</sub> at pH 7, 1 g/L adsorbent dosage and 25 mg/L initial vancomycin concentration. Results of comparative experiments are illustrated in Fig. 3. Accordingly, by increasing contact time, a sharp enhancement was observed in vancomycin adsorptive removal using three different adsorbents. Furthermore, among all the applied adsorbents, Fe<sub>3</sub>O<sub>4</sub> showed lowest antibiotic removal efficiency with about 19.20%, after 120 min contact time. However, impregnation of PAC with nanoparticles led to the significant improvement of vancomycin removal to around 89.58%. This result confirms the effect of PAC on the better dispersion of Fe<sub>3</sub>O<sub>4</sub> in the solution and also increasing the reactive surface areas required for vancomycin adsorption.

#### 3.2. Effect of experimental variables

##### 3.2.1. Effect of solution pH

pH of aqueous solution has a significant effect on the interaction between adsorbents and adsorbates, due to its influence on surface charge, protonation and functional groups onto the surfaces of adsorbents. Therefore, in the present research, the effect of solution pH on antibiotic adsorptive removal onto the PAC/Fe<sub>3</sub>O<sub>4</sub> was carried out at pH range of 3–11, 1 g/L adsorbent dosage and 120 min contact time. Fig. 4 shows the effect of pH of solution on antibiotic removal. Accordingly, the maximum amount of antibiotic adsorptive removal was obtained at pH of 5 (97.83%), while the minimum adsorption was obtained at pH of 3 with only 58.74%. Previous research has shown that the optimum pH range for antibiotic removal is around 5–7 [5,13]. The relationship between the adsorbent and adsorbate molecules can be justified by the adsorbent surface charge and the dissociation constant (PKa) of PAC/Fe<sub>3</sub>O<sub>4</sub>. pHzpc of vancomycin molecules is in the range of 5–7 which indicates that they are protonated at pH < 5. But, at pH range of 5 to 7.5, vancomycin molecules are neutral and can be adsorbed electrostatically onto the surfaces of activated carbon, while at pH > 7, the anionic forms of vancomycin are common. Moreover, the isoelectric point of magnetite is 7 ± 0.2 [38], indicates that the adsorbent charges at acidic pH values are positive and at alkaline pH values are negative [39]. One of the most possible reasons for adsorbing vancomycin at pH 5 is electrostatic repulsive forces between adsorbent and adsorbate molecules at the other pH values. Therefore, the

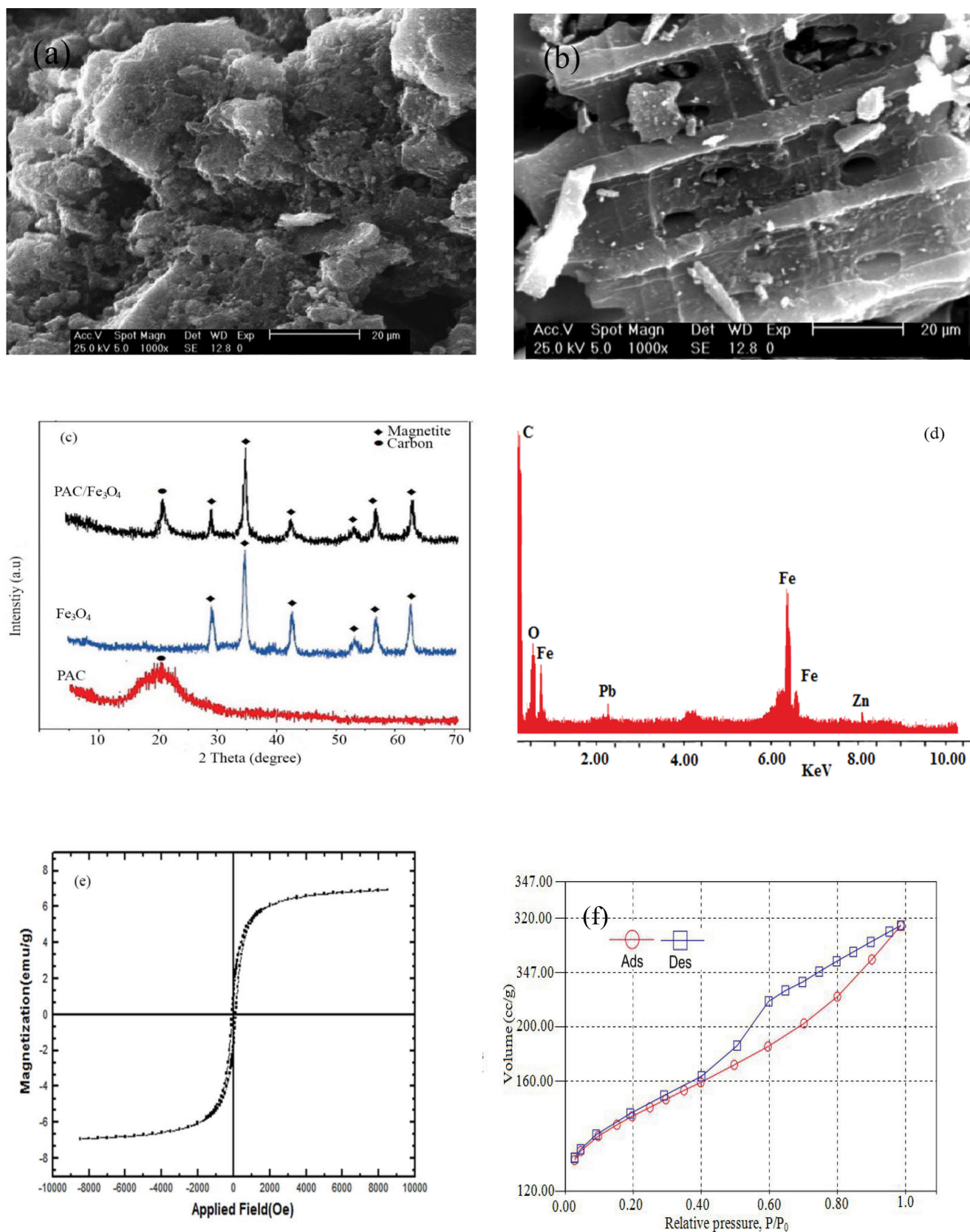


Fig. 2. SEM images of (a) pure PAC and (b) PAC/MNPs, XRD diagrams of PAC, Fe<sub>3</sub>O<sub>4</sub> and (c), EDAX spectrum (d), magnetization curve of PAC/Fe<sub>3</sub>O<sub>4</sub> (e) and BET diagrams of PAC/Fe<sub>3</sub>O<sub>4</sub> (f).

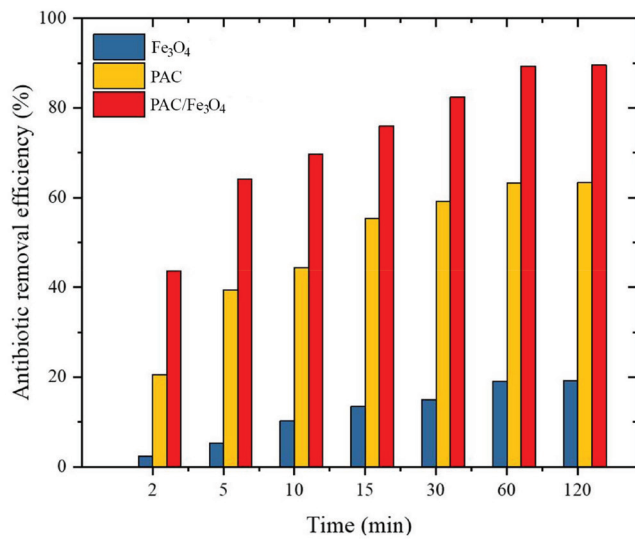


Fig. 3. A comparative study of vancomycin adsorption onto the surfaces of PAC, Fe<sub>3</sub>O<sub>4</sub> and PAC/Fe<sub>3</sub>O<sub>4</sub>. (pH of solution: 7, Contact time: 120 min, adsorbent dosage: 1 g/L and initial vancomycin concentration: 25 mg/L).

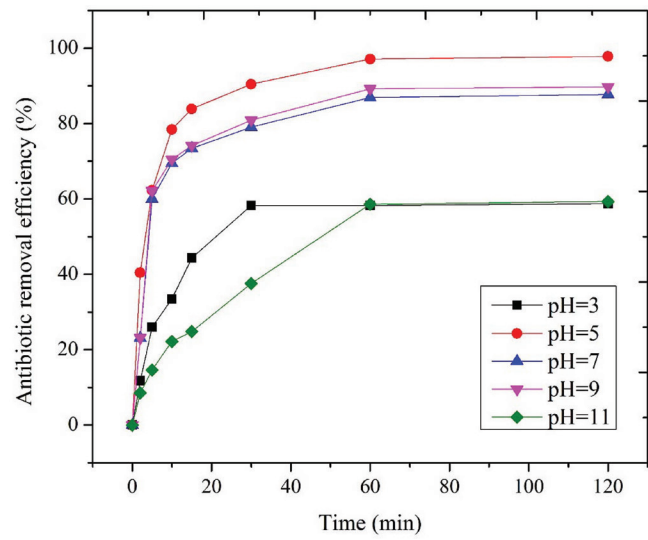


Fig. 4. Effect of solution pH on vancomycin adsorption onto the surfaces of PAC/Fe<sub>3</sub>O<sub>4</sub> (contact time: 120 min, adsorbent dosage: 1 g/L and initial vancomycin concentration: 25 mg/L).

highest vancomycin adsorptive removal was obtained at pH 5, while the lowest removal was observed at pH 3 and 8.

Reaction time is one of the most essential parameters in designing a typical batch system. So, several experiments were done within a 120 min time period at different time intervals by keeping the other variables constant. Fig. 4 illustrates vancomycin adsorption at different pH values during 120 min. Having a closer look, vancomycin removal efficiency showed an increasing trend by increasing reaction time. Indeed, by enhancement in time intervals to 60 min, antibiotic removal efficiency reached to the maximum but after that no significant changes were observed. Therefore, 60 min was selected as an optimum reaction time for vancomycin removal and also used in the subsequent experiments. High vancomycin adsorption at first 60 min of reaction can be ascribed to the high vacant sites onto the surfaces of adsorbent that create high affinity towards adsorption of molecules. However, as contact time increased, adsorbate attachment onto the surface sites decreased, due to their filling by adsorbate molecules and reach to the equilibrium state. Results of Wang et al. [40] about the application of magnetic resin adsorbent on three antibiotics removal from aqueous solution revealed that most of antibiotics were removed at first 10 min which was equilibrated until 30 min. Furthermore, Zhang et al. [41] reported that the equilibrium contact time for adsorptive removal of 28 antibiotics using AC was 120 min.

### 3.2.2. Effect of adsorbent dosages and initial antibiotic concentrations

Adsorbent dosage is a critical input variable in batch experiments with a significant role on adsorption capacity. So, in this study, various adsorbent dosages (0.1–2 g/L)

were used to find the optimum amount of adsorbent for vancomycin adsorptive removal. Fig. 5 shows that a direct relationship was observed between the adsorbent dosage and vancomycin adsorptive removal. When adsorbent dosage increased from 0.1 to 2 g/L, antibiotic removal efficiency showed an enhancing trend from 22.50 to 96.43%. Therefore, 2 g/L was selected as an equilibrium adsorbent dosage and applied for the next batch experiments. This finding would be ascribed to the fact that increasing adsorbent dosage led to the enhancement of vacant reactive sites onto the surfaces of adsorbents that may cause an increase in their ability to adsorb more adsorbate

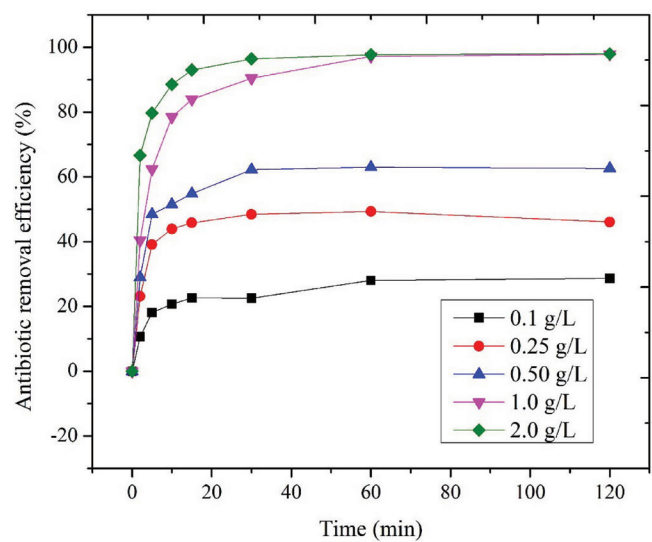


Fig. 5. Effect of different adsorbent dosages on antibiotic adsorption onto the surfaces of PAC/Fe<sub>3</sub>O<sub>4</sub> (pH of solution: 5, contact time: 60 min and initial vancomycin concentration: 25 mg/L).

molecules [42]. Findings of Kakavandi et al. [43] showed that by increasing magnetic activated carbon dosage from 1 to 5 g/L, the removal efficiency of amoxicillin showed an enhancing trend. Similar results have been reported by previous researchers in the literature [44,45].

Fig. 6 illustrates antibiotic removal using PAC/Fe<sub>3</sub>O<sub>4</sub> under various initial antibiotic concentrations at pH 5 and 2 g/L adsorbent dosage. Based on the figure, an indirect relationship was observed between initial antibiotic concentrations and antibiotic removal efficiency. As can be seen from Fig. 6, since initial antibiotic concentration increased from 10 to 100 mg/L, antibiotic removal efficiency declined from 96.59 to 68.20%. This observation can be related to the ratio of fixed number of reactive sites onto the surfaces of adsorbent versus pollutant molecules. When the number of adsorbate molecules increases, more reactive sites will be occupied by adsorbate molecules that prevent subsequent pollutant adsorption [46,47]. In the study of Samarghandi et al. [48] on adsorptive removal of cephalexin using zeolite and zeolite-stabilized manganese oxide nanoparticles, a sharp decrease was observed in cephalexin removal efficiency by an increase in its concentration from 10 to 40 mg/L.

### 3.3. Isotherm and kinetic studies

#### 3.3.1. Isotherm modeling

The adsorption of antibiotic onto the surfaces of PAC/Fe<sub>3</sub>O<sub>4</sub> was modeled using four isotherm models namely, Langmuir, Freundlich, Temkin and Dubinin-Radushkevich (D-R) and the quality of fitness was evaluated using coefficient of correlation ( $R^2$ ). Table 1 illustrates the obtained constants and related coefficients of correlation of each applied model. Fig. 7a shows linear graph of Langmuir model where the intercept and slope of this graph were applied to find  $q_e$  and  $K_L$ , respectively. Furthermore, Freundlich isotherm graph was plotted in Fig. 7b which

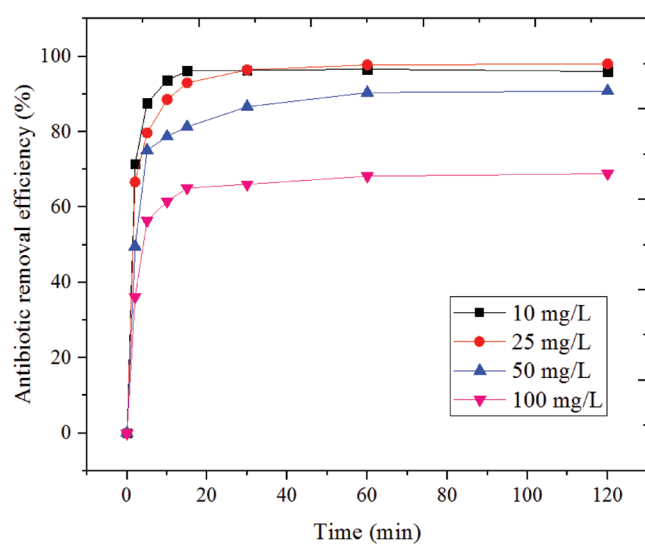


Fig. 6. Effect of different initial antibiotic concentrations on antibiotic adsorption onto the surfaces of PAC/Fe<sub>3</sub>O<sub>4</sub> (pH of solution: 5, contact time: 60 min and adsorbent dosage: 1 g/L).

was used for finding  $K_F$  and  $n$  based on slope and intercept of graph, respectively. Fig. 7c also shows linear graph of Temkin model to find  $\beta$  and  $q_d$  from the slope and intercept, respectively. Finally, the slope and intercept of linear graph (Fig. 7d) of D-R model was used to obtain  $\beta$  and  $q_d$  model parameters, respectively. The validity of each applied isotherm model was tested using coefficient of correlation ( $R^2$ ). According to Table 1, the highest coefficient of correlation belongs to Freundlich model indicating its highest correlation with the experimental data, compared to the other applied models. Fu et al. [49] reported that Freundlich isotherm model showed highest correlation with the experimental data of quinolone antibiotics onto the surfaces of activated carbon. Furthermore, isotherm models with  $n > 1$  are categorized as L-type isotherms indicating an extensive inclination of adsorbent to the adsorbate which is indicative of their chemisorption nature [50]. Moreover, the obtained RL constant of Langmuir model shows that the experimental conditions of adsorption were favorable. Table 2 shows several maximum adsorption capacities of antibiotic removal onto the surfaces of different adsorbents. Accordingly, it can be concluded that PAC/Fe<sub>3</sub>O<sub>4</sub> is an efficient adsorbent with relatively high adsorption capacity, compared to the other studied adsorbents, to remove vancomycin from aqueous solution. The obtained adsorption capacity of D-R model was not consistent with  $q_m$  determined by Langmuir model. Since, the coefficient of correlation of D-R was significantly lower than the other models, it is concluded that the adsorption of vancomycin on PAC/Fe<sub>3</sub>O<sub>4</sub> did not follow a physical process.

#### 3.3.2. Kinetic modeling

Kinetic study of antibiotic adsorption onto the PAC/Fe<sub>3</sub>O<sub>4</sub> surfaces was studied through fitting the experimental data of vancomycin removal on four

Table 1  
Isotherm parameters of antibiotic adsorption onto the surfaces of PAC/Fe<sub>3</sub>O<sub>4</sub>

Model	Parameter	Value
Langmuir	$q_m$ (mg/g)	66.67
	$K_L$ (L/mg)	0.17
	$R_L$	0.2
	$R^2$	0.853
Freundlich	$k_f$ (mg/g(L mg) <sup>1/n</sup> )	12.94
	$n$ (-)	2.14
	$R^2$	0.953
Temkin	$K_t$ (mg g <sup>-1</sup> min <sup>-0.5</sup> )	1
	$B$	12.6
	$R^2$	0.880
Dubinin-Radushkevich	$\beta$	0.0035
	$q_m$ (mg/g)	38.51
	$R^2$	0.786

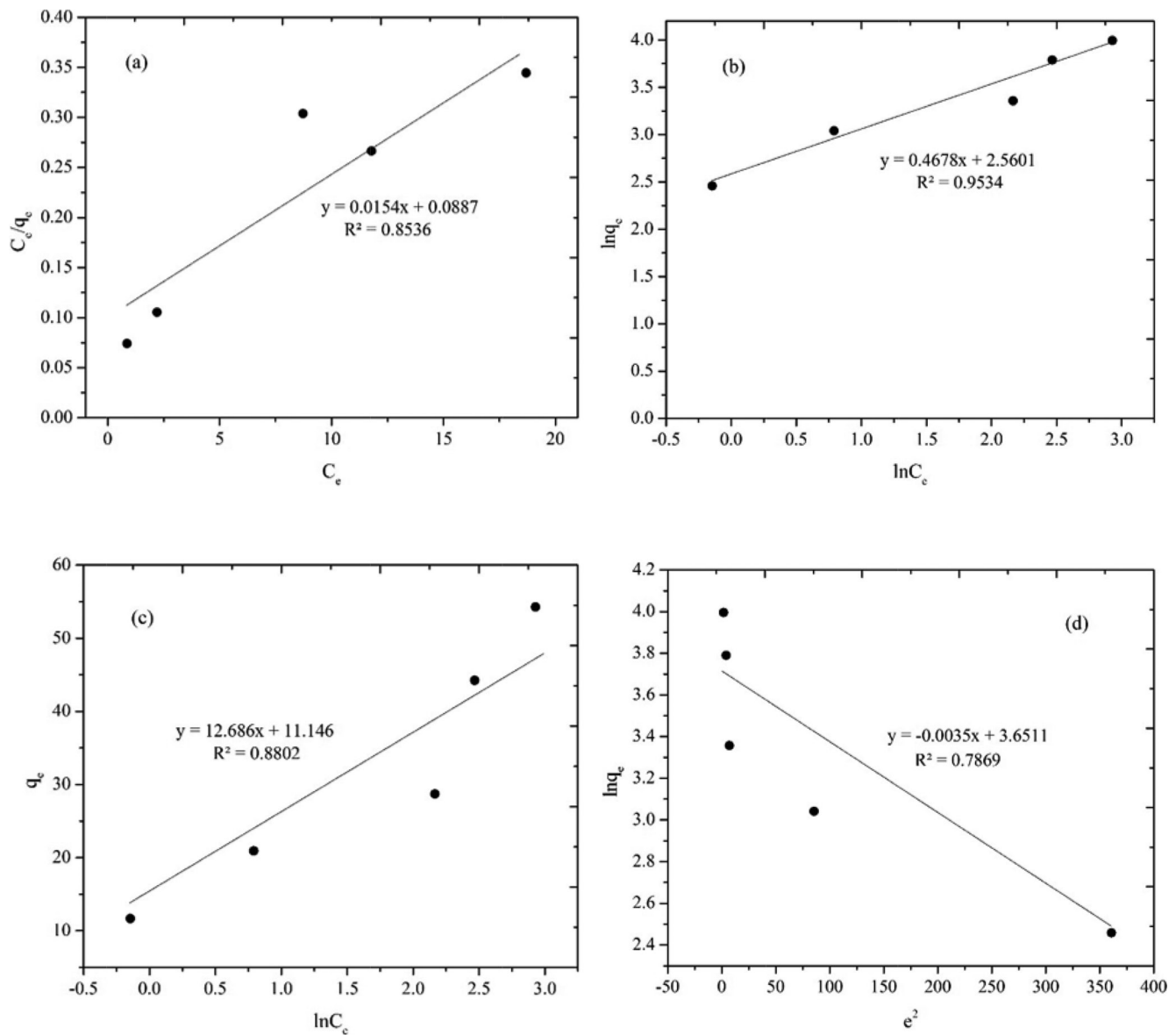


Fig. 7. Linearization of (a) Langmuir, (b) Freundlich, (c) Temkin and (d) Dubinin-Radushkevich isotherm models.

kinetic models including pseudo first-order, pseudo second-order, elovich and intraparticle diffusion at different initial antibiotic concentrations. The obtained kinetic parameters and coefficients of correlation are demonstrated in Table 3. The plot of  $\ln(q_e - q_t)$  vs. time for the pseudo first-order model is illustrated in Fig. 8a for finding  $q_e$  and  $k_1$  from slope and intercept of the graph, respectively. Furthermore, pseudo-second-order graph (Fig. 8b) is plotted based on  $t/q$  against time to determine  $q_e$  and  $k_2$  based on slope and intercept, respectively. The elovich linear plot of  $q_t$  against  $\ln t$  is also shown in Fig. 8c for obtaining  $k_T$  and  $\beta$  from the slope and intercept, respectively. Finally, Fig. 8d was plotted for intraparticle diffusion model by  $q_t$  vs  $t^{1/2}$  for determining  $k_i$  and  $C$  from slope and intercept, respectively. Having a closer look to Table 3, equilibrium adsorption constant of pseudo first-

order model showed an increasing trend with enhancing initial antibiotic concentrations. Accordingly, with an enhancement in initial antibiotic concentrations from 10 to 100 mg/L,  $q_e$  rose from 3.32 to 11.44 mg/g. In addition, similar trend was observed for equilibrium adsorption constant of pseudo second-order model. Moreover, within a similar increase in initial antibiotic concentration, a sharp increase was happened in  $q_e$  from 4.95 to 34.48 mg/g. The experimental adsorption capacity ( $q_e, \text{exp}$ ) obtained by pseudo-first-order and pseudo second-order models are reported in Table 3. Accordingly, the obtained  $q_e, \text{exp}$  of pseudo second-order model have more correlation with fitted adsorption capacity, compared to the pseudo first-order model. Moreover, among the studied models, pseudo second-order had the highest coefficient of correlation (>0.99) than the other models which shows the

Table 2  
Comparison of the maximum adsorption capacities of the reported adsorbents towards some typical antibiotics in literatures

Antibiotic	Adsorbent	Equilibrium adsorption (mg/g)	Reference
Flumequine	Glycerol-based carbon material	0.69	Álvarez-Torrellas et al., [51]
Tetracycline		31.69	
Oxytetracycline	Vermiculite	36.80	Liu et al., [52]
Ciprofloxacin		36.87	
Cefradine	CdS-MWCNT	40.525	Fakhri et al., [53]
Enrofloxacin	Mesoporous silica	6.23	Liang et al., [54]
Quinolone	KGa-1b	1.03	Wu et al., [55]
	SAz-1	24	
Vancomycin	PAC/Fe <sub>3</sub> O <sub>4</sub>	66.67	This study

Table 3  
Kinetic adsorption data for antibiotic removal using PAC/Fe<sub>3</sub>O<sub>4</sub>

Model	Parameter	Value			
		Initial antibiotic concentrations (mg/L)			
		10	25	50	100
Pseudo-first order	$K_1$ (1/min)	0.815	0.202	0.179	0.153
	$q_e$ (mg/g)	3.32	4.09	10.17	11.44
	$q_t$ (mg/g)	4.58	11.41	21.71	33.85
	$R^2$	0.954	0.913	0.925	0.830
Pseudo-second order	$K_2$ (g/mg.min)	0.412	0.072	0.027	0.02
	$q_e$ (mg/g)	4.95	12.19	21.73	34.48
	$q_t$ (mg/g)	4.58	11.41	21.71	33.85
	$R^2$	0.9999	1	0.9997	0.9998
Intraparticle diffusion	$K_i$ (mg/g.min <sup>-0.5</sup> )	0.489	1.24	2.36	3.74
	$C$ (–)	2.23	4.77	7.68	12
	$R^2$	0.506	0.592	0.645	0.634
Elovich	$K_e$ (mg/g.min)	1.42	3.06	13.6	70.8
	$\beta$ (g/mg)	3.69	7.74	11.9	18.3
	$R^2$	0.761	0.917	0.852	0.808

best fit with the experimental data of antibiotic adsorption. Results of Ahmed et al. [56] and Zhang et al. [41] on adsorptive removal of some antibiotics with different adsorbents showed that pseudo second-order model was the best kinetic model to fit the data of antibiotics removal. The findings reveal that the adsorption process was based on the quantity of adsorbed solute onto the surfaces of the adsorbent and the quantity of adsorbed solute at equilibrium state. Furthermore, intraparticle diffusion model was used to find the dominant mechanism of adsorption and rate controlling step. Based on Table 3, low amount of  $R^2$  for all initial vancomycin concentrations revealed that this model did not appropriately fit the adsorption data of antibiotic onto the surfaces of PAC/Fe<sub>3</sub>O<sub>4</sub>. Hence, it is obvious that intraparticle diffusion was not the main mechanism in vancomycin adsorptive

removal. So, the other possible mechanisms like ion-exchange and complexes played an important role in adsorbing vancomycin on the synthesized composite.

### 3.4. Regeneration studies

The reusability experiments were performed for finding the efficiency of adsorbent after use. Fig. 9 shows the results of reusability experiments of PAC/Fe<sub>3</sub>O<sub>4</sub> after five cycles of use. Accordingly, a slight decrease was observed in vancomycin removal efficiency after five consecutive cycles of use. The most probable reason to justify decreasing adsorbent efficiency would be the filling of adsorbent surface pores with adsorbate molecules. Based on the figure, antibiotic removal efficiency declined from 92.80% at the first cycle to 63.53% at the fifth cycle.

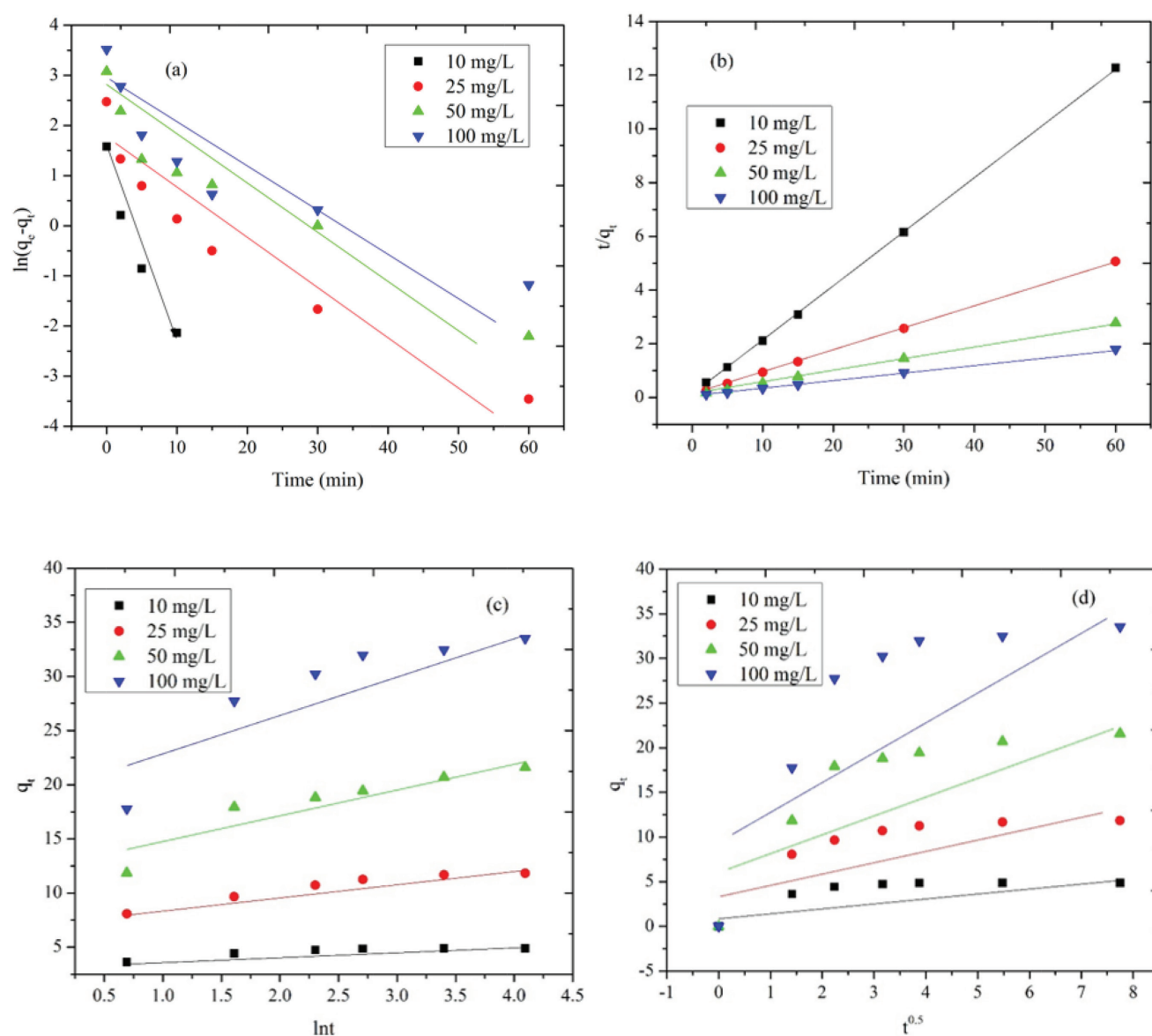


Fig 8. Linearization of (a) Pseudo first-order, (b) Pseudo second-order, (c) Elovich and (d) Intraparticle diffusion kinetic models.

However, after passing three cycles of use, antibiotic removal efficiency just decreased from 92.80 to over 80%, indicating high ability of adsorbent to remove antibiotic, even after three cycles of use.

#### 4. Conclusion

Antibiotic vancomycin removal was carried out in a batch system under different experimental variables. Results showed that increasing adsorbent dosage and contact time led to a significant enhancement in vancomycin removal. While, increasing initial antibiotic concentrations caused a decrease in the removal of antibiotic. In general, maximum antibiotic removal was obtained at pH 5, 60 contact time and 2 g/L adsorbent dosage. The obtained

results of isotherm and kinetic studies revealed that among all the applied models, the experimental data of antibiotic adsorptive removal had the highest compatibility with Freundlich isotherm model and pseudo second-order kinetic model. Additionally, from the obtained results of this study, it can be postulated that PAC/Fe<sub>3</sub>O<sub>4</sub> is a promising and efficient composite that not only had high capability of adsorbing antibiotic, but also can easily be separated by means of an external magnet.

#### Acknowledgment

This article was derived from M.Sc. degree thesis of Miss. Forough Gashtasbi which was performed under supervision of Dr. Reza Jalilzadeh at the Department of

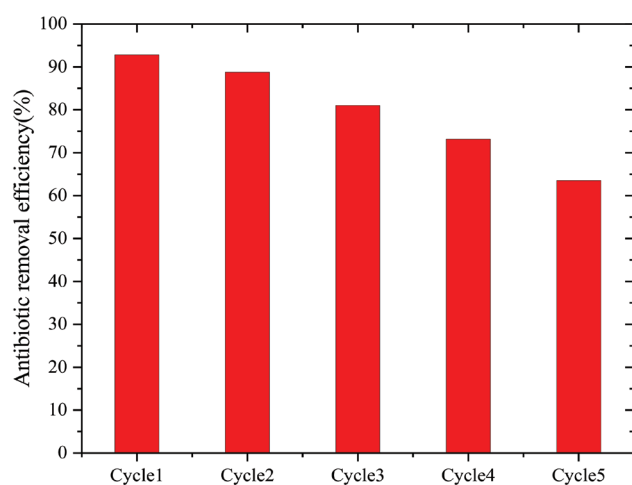


Fig. 9. Reusability of PAC/Fe<sub>3</sub>O<sub>4</sub> after five cycles of adsorption/desorption.

Environmental Engineering, Ahvaz Branch, Islamic Azad University, Iran. The authors of this paper are sincerely grateful to Ahvaz Jundishapur University of Medical Sciences Dr. Ali Akbar Babaei for their academic support.

## References

- [1] X. Chang, M.T. Meyer, X. Liu, Q. Zhao, H. Chen, J.A. Chen, W. Shu, Determination of antibiotics in sewage from hospitals, nursery and slaughter house, wastewater treatment plant and source water in Chongqing region of Three Gorge Reservoir in China, *Environ. Pollut.*, 158 (2010) 1444–1450.
- [2] N. Alavi, A.A. Babaei, M. Shirmardi, A. Naimabadi, G. Goudarzi, Assessment of oxytetracycline and tetracycline antibiotics in manure samples in different cities of Khuzestan Province, Iran, *Environ. Sci. Pollut. Res.*, 22 (2015) 17948–17954.
- [3] R. Hirsch, T. Ternes, K. Haberer, K.L. Kratz, Occurrence of antibiotics in the aquatic environment, *Sci. Total. Environ.*, 225 (1999) 109–118.
- [4] J. Rivera-Utrilla, G. Prados-Joya, M. Sánchez-Polo, M.A. Ferro-García, I. Bautista-Toledo, Removal of nitro imidazole antibiotics from aqueous solution by adsorption/bioadsorption on activated carbon, *J. Hazard. Mater.*, 170 (2009) 298–305.
- [5] H. Liu, W. Liu, J. Zhang, C. Zhang, L. Ren, Y. Li, Removal of cephalixin from aqueous solutions by original and Cu (II)/Fe (III) impregnated activated carbons developed from lotus stalks Kinetics and equilibrium studies, *J. Hazard. Mater.*, 185 (2011) 1528–1535.
- [6] K. Kummerer, A. Al-Ahmad, V. Mersch-Sundermann, Biodegradability of some antibiotics, elimination of the genotoxicity and affection of wastewater bacteria in a simple test, *Chemosphere*, 40 (2000) 701–710.
- [7] M.S. Diaz-Cruz, D. Barceló, LC–MS 2 trace analysis of antimicrobials in water, sediment and soil, *Trac-Trends. Anal. Chem.*, 24 (2005) 645–657.
- [8] A. Gobel, A. Thomsen, C.S. McArdell, A. Joss, W. Giger, Occurrence and sorption behavior of sulfonamides, macrolides, and trimethoprim in activated sludge treatment, *Environ. Tci. Technol.*, 39 (2005) 3981–3989.
- [9] A. Gulkowska, H.W. Leung, M.K. So, S. Taniyasu, N. Yamashita, L.W. Yeung, P.K. Lam, Removal of antibiotics from wastewater by sewage treatment facilities in Hong Kong and Shenzhen, China, *Water. Res.*, 42 (2008) 395–403.
- [10] Z. Bai, Q. Yang, J. Wang, Catalytic ozonation of sulfamethazine antibiotics using Ce 0.1 Fe 0.9 OOH: Catalyst preparation and performance, *Chemosphere*, 161 (2016) 174–180.
- [11] N.F. Moreira, J.M. Sousa, G. Macedo, A.R. Ribeiro, L. Barreiros, M. Pedrosa, C.M. Manaia, Photocatalytic ozonation of urban wastewater and surface water using immobilized TiO<sub>2</sub> with LEDs: Micropollutants, antibiotic resistance genes and estrogenic activity, *Water. Res.*, 94 (2016) 10–22.
- [12] H. Niu, Z. Meng, Y. Cai, Fast defluorination and removal of norfloxacin by alginate/Fe@ Fe<sub>3</sub>O<sub>4</sub> core/shell structured nanoparticles, *J. Hazard. Mater.*, 227 (2012) 195–203.
- [13] J.A. de Lima Perini, M. Perez-Moya, R.F.P. Nogueira, Photo-Fenton degradation kinetics of low ciprofloxacin concentration using different iron sources and pH, *J. Photochem. Photobiol. A.*, 259 (2013) 53–58.
- [14] L. Demarchis, M. Minella, R. Nisticò, V. Maurino, C. Minero, D. Vione, Photo-Fenton reaction in the presence of morphologically controlled hematite as iron source, *J. Photochem. Photobiol. A.*, 307 (2015) 99–107.
- [15] X.Q. Cheng, C. Zhang, Z.X. Wang, L. Shao, Tailoring nanofiltration membrane performance for highly-efficient antibiotics removal by mussel-inspired modification, *J. Membr. Sci.*, 499 (2016) 326–334.
- [16] A.A. Babaei, E.C. Lima, A. Takdastan, N. Alavi, G. Goudarzi, M. Vosoughi, M. Shirmardi, Removal of tetracycline antibiotic from contaminated water media by multi-walled carbon nanotubes: operational variables, kinetics, and equilibrium studies, *Water. Sci. Technol.*, 74 (2016) 1202–1216.
- [17] L. Xu, J. Dai, J. Pan, X. Li, P. Huo, Y. Yan, R. Zhang, Performance of rattle-type magnetic mesoporous silica spheres in the adsorption of single and binary antibiotics, *Chem. Eng. J.*, 174 (2011) 221–230.
- [18] K. Li, A. Yediler, M. Yang, S. Schulte-Hostede, M.H. Wong, Ozonation of oxytetracycline and toxicological assessment of its oxidation by-products, *Chemosphere*, 72 (2008) 473–478.
- [19] A.G. Trovo, R.F.P. Nogueira, A. Agüera, A.R. Fernandez-Alba, S. Malato, Degradation of the antibiotic amoxicillin by photo-Fenton process—chemical and toxicological assessment, *Water Res.*, 45 (2011) 1394–1402.
- [20] S. Lenore, E. Arnold, D. Andrew, eds., *Standardized Methods of Water Examination*, Washington, 41 (1998) 531–546.
- [21] A.A. Babaei, Z. Alaei, E. Ahmadpour, A. Ramazanpour-Esfahani, Kinetic modeling of methylene blue adsorption onto acid-activated spent tea: A comparison between linear and non-linear regression analysis, *J. Adv. Environ. Health. Res.*, 2 (2014) 197–208.
- [22] H.R. Pourtedal, N. Sadegh, Effective removal of amoxicillin, cephalixin, tetracycline and penicillin G from aqueous solutions using activated carbon nanoparticles prepared from vine wood, *J. Water. Process. Eng.*, 1 (2014) 64–73.
- [23] J. Rivera-Utrilla, C.V. Gómez-Pacheco, M. Sánchez-Polo, J. López-Peñalver, R. Ocampo-Pérez, Tetracycline removal from water by adsorption/bioadsorption on activated carbons and sludge-derived adsorbents, *J. Environ. Manage.*, 131 (2013) 16–24.
- [24] M.S. Legnoverde, S. Simonetti, E.I. Basaldella, Influence of pH on cephalixin adsorption onto SBA-15 mesoporous silica: Theoretical and experimental study, *App. Surf. Sci.*, 300 (2014) 37–42.
- [25] B. Kakavandi, A. Takdastan, N. Jaafarzadeh, M. Azizi, A. Mirzaei, A. Azari, Application of Fe<sub>3</sub>O<sub>4</sub>@ C catalyzing heterogeneous UV-Fenton system for tetracycline removal with a focus on optimization by a response surface method, *J. Photochem. Photobiol. A.*, 314 (2016) 178–188.
- [26] A.A. Babaei, M. Bahrami, A. Farrokhan Firouzi, A. Ramazanpour Esfahani and L. Alidokht, Adsorption of cadmium onto modified nanosized magnetite: kinetic modeling, isotherm studies, and process optimization, *Desal. Water Treat.*, 56 (2015) 3380–3392.
- [27] A. Ramazanpour Esfahani, A. Farrokhan Firouzi, Synthesis and application of stabilized zero-valent iron nanoparticles for hexavalent chromium removal in saturated sand columns:

- experimental and modeling studies, *Desal. Water Treat.*, 57 (2016) 15424–15434.
- [28] M.H. Do, N.H. Phan, T.D. Nguyen, T.T.S. Pham, V.K. Nguyen, T.T.T. Vu, T.K.P. Nguyen, Activated carbon/Fe<sub>3</sub>O<sub>4</sub> nanoparticle composite: fabrication, methyl orange removal and regeneration by hydrogen peroxide, *Chemosphere*, 85 (2011), 1269–1276.
- [29] F. Çeçen, O. Aktas, eds., *Activated Carbon for Water and Wastewater Treatment: Integration of Adsorption and Biological Treatment*, Wiley, 2011, pp. 13–37.
- [30] T.W. Weber, R.K. Chakravorti, Pore and solid diffusion models for fixed-bed adsorbers, *AI. Che. J.*, 20 (1974) 228–238.
- [31] M.I. Temkin, V. Pyzhev, Kinetics of ammonia synthesis on promoted iron catalysts, *Actaphysiochim.*, 12 (1940) 217–222.
- [32] N.D. Hutson, R.T. Yang, Theoretical basis for the Dubinin-Radushkevitch (DR) adsorption isotherm equation, *Adsorption*, 3 (1997) 189–195.
- [33] S. Lagergren, Zurtheorie der sogenannten adsorption gelosterstoffe. *Kungliga Svenska Vetenskapsakademiens, Handlingar.*, 24 (1898) 1–39.
- [34] Y.S. Ho, G. McKay, Pseudo-second order model for sorption processes, *Process Biochem.*, 34 (1999) 451–465.
- [35] I.A.W. Tan, A.L. Ahmad, B.H. Hameed, Adsorption isotherms, kinetics, thermodynamics and desorption studies of 2, 4, 6-trichlorophenol on oil palm empty fruit bunch-based activated carbon, *J. Hazard. Mater.*, 164 (2009) 473–482.
- [36] Z. Liu, F.S. Zhang, R. Sasai, Arsenate removal from water using Fe<sub>3</sub>O<sub>4</sub>-loaded activated carbon prepared from waste biomass, *Chem. Eng. J.*, 160 (2010) 157–162.
- [37] N. Yang, S. Zhu, D. Zhang, S. Xu, Synthesis and properties of magnetic Fe<sub>3</sub>O<sub>4</sub>-activated carbon nanocomposite particles for dye removal, *Mater. Lett.*, 62 (2008) 645–657.
- [38] B. Kakavandi, M. Jahangirrad, M. Rafiee, A.R. Esfahani, A.A. Babaei, Development of response surface methodology for optimization of phenol and p-chlorophenol adsorption on magnetic recoverable carbon, *Micropor. Mesopor. Mater.*, 231 (2016) 192–206.
- [39] E. Çalıkan, S. Goktürk, Adsorption characteristics of sulfamethoxazole and metronidazole on activated carbon, *Separ. Sci. Technol.*, 45 (2010) 244–255.
- [40] T. Wang, X. Pan, W. Ben, J. Wang, P. Hou, Q. Zhimin, Adsorptive removal of antibiotics from water using magnetic ion exchange resin, *J. Environ. Sci.*, 52 (2017) 111–117.
- [41] X. Zhang, W. Guo, H.H. Ngo, H. Wen, N. Li, W. Wu, Performance evaluation of powdered activated carbon for removing 28 types of antibiotics from water, *J. Environ. Manage.*, 172 (2016) 193–200.
- [42] S.A. Umoren, U.J. Etim, A.U. Israel, Adsorption of methylene blue from industrial effluent using poly (vinyl alcohol), *J. Mater. Environ. Sci.*, 4 (2013) 75–86.
- [43] B. Kakavandi, A. Esrafil, A. Mohseni-Bandpi, A.J. Jafari, R.R. Kalantary, Magnetic Fe<sub>3</sub>O<sub>4</sub>@C nanoparticles as adsorbents for removal of amoxicillin from aqueous solution, *Water Sci. Technol.*, 69 (2014) 147–155.
- [44] M. Hadavifar, M. Bahramifar, H. Younesi, M. Rastakhiz, Q. Li, J. Yu, E. Eftekhari, Removal of mercury (II) and cadmium (II) ions from synthetic wastewater by a newly synthesized amino and thiolated multi-walled carbon nanotubes, *J. Taiwan. Inst. Chem. Eng.*, 67 (2016) 397–405.
- [45] G. Nazari, H. Abolghasemi, M. Esmaili, Batch adsorption of cephalexin antibiotic from aqueous solution by walnut shell-based activated carbon, *J. Taiwan. Inst. Chem. Eng.*, 58 (2016) 357–365.
- [46] K.Y. Chen, J.C. Liu, P.N. Chiang, S.L. Wang, W.H. Kuan, Y.M. Tzou, M.K. Wang, Chromate removal as influenced by the structural changes of soil components upon carbonization at different temperatures, *Environ. Pollut.*, 162 (2012) 151–158.
- [47] A. Ali, K. Saeed, F. Mabood, Removal of chromium (VI) from aqueous medium using chemically modified banana peels as efficient low-cost adsorbent, *Alex. Eng. J.*, 3 (2016) 2933–2942.
- [48] M.R. Samarghandi, T.J. Al-Musawi, A. Mohseni-Bandpi, M. Zarrabi, Adsorption of cephalexin from aqueous solution using natural zeolite and zeolite coated with manganese oxide nanoparticles, *J. Mol. Liq.*, 211 (2015) 431–441.
- [49] H. Fu, X. Li, J. Wang, P. Lin, C. Chen, X. Zhang, I.H. Suffet, Activated carbon adsorption of quinolone antibiotics in water: Performance, mechanism, and modeling, *J. Environ. Sci.*, 56 (2017) 145–152.
- [50] M.R. Taha, K. Ahmad, A.A. Aziz, Z. Chik, B.B.K. Huat, G.S. Sew, F.H. Ali, Geo environmental aspects of tropical residual soils, *Trop. Residual. Soils. Eng.*, (2004) 213–229.
- [51] S. Alvarez-Torrellas, R.S. Ribeiro, H.T. Gomes, G. Ovejero, J. Garcia, Removal of antibiotic compounds by adsorption using glycerol-based carbon materials, *Chem. Eng. J.*, 2016 (296) 277–288.
- [52] S. Liu, P. Wu, L. Yu, L. Li, B. Gong, N. Zhua, Z. Dang, C. Yang, Preparation and characterization of organo-vermiculite based on phosphatidylcholine and adsorption of two typical antibiotics, *Appl. Clay. Sci.*, 137 (2017) 160–167.
- [53] A. Fakhri, S. Rashidi, M. Asif, I. Tyagi, S. Agarwal, V.K. Gupta, Dynamic adsorption behavior and mechanism of cefotaxime, cefradine and cefazolin antibiotics on CdS-MWCNT nano composites, *J. Mol. Liq.*, 215 (2016) 269–275.
- [54] Z. Liang, Z. Zhao, T. Sun, W. Shi, F. Cui, Adsorption of quinolone antibiotic in spherical mesoporous silica, *J. Hazard. Mater.*, 2016 (15) 8–14.
- [55] Q. Wu, Z. Li, H. Hong, Adsorption of the quinolone antibiotic nalidixic acid onto montmorillonite and kaolinite, *Appl. Clay. Sci.*, 74 (2013) 66–73.
- [56] M.B. Ahmed, J.L. Zhou, H.H. Ngo, W. Guo, Adsorptive removal of antibiotics from water and wastewater: progress and challenges. *Sci. Total. Environ.*, 532 (2015) 112–126.